Engineered Biosynthesis of the Antiparasitic Agent Frenolicin B and Rationally Designed Analogs in a Heterologous Host

Jay T. Fitzgerald[†], **Christian P. Ridley**[†,§], and **Chaitan Khosla**[†,‡,*]

[†]Department of Chemistry, Stanford University, California 94305

[‡]Department of Chemical Engineering, Stanford University, California 94305

Abstract

The polyketide antibiotic frenolicin B harbors a biosynthetically intriguing benzoisochromanequinone core, and has been shown to exhibit promising antiparasitic activity against *Eimeria tenella*. To facilitate further exploration of its chemistry and biology, we constructed a biosynthetic route to frenolicin B in the heterologous host *Streptomyces coelicolor* CH999, despite the absence of key enzymes in the identified frenolicin gene cluster. Together with our understanding of the underlying polyketide biosynthetic pathway, this heterologous production system was exploited to produce analogs modified at the C15 position. Both the natural product and these analogs inhibited the growth of *Toxoplasma gondii* in a manner that reveals sensitivity to the length of the C15 substituent. The ability to construct a functional biosynthetic pathway, despite a lack of genetic information, illustrates the feasibility of a modular approach to engineering medicinally relevant polyketide products.

Introduction

Type II polyketide synthases (PKSs) catalyze the biosynthesis of the carbon skeletons of numerous polyfunctional aromatic natural products from the actinomycetes, including the clinically important antibiotic oxytetracycline and the anticancer agent doxorubicin [1,2]. Recent analysis has demonstrated considerable functional modularity within these multienzyme assemblies, which in turn can be exploited to alter priming units and change polyketide backbone length [3,4]. At the same time, the substrate flexibility of late-stage tailoring enzymes in these natural product pathways can also be exploited to create designer molecules [4,5]. Here we have harnessed each of these modular elements to reconstruct a chimeric pathway to the antiparasitic antibiotic frenolicin B (**1b**) as well as targeted analogs in a heterologous host. Biological evaluation of our analogs against *Toxoplasma gondii* has revealed the strong sensitivity of this family of antibiotics to the identity of the C-15 substituent, thereby highlighting a new direction for future antiparasitic drug design.

[*]To whom correspondence should be addressed. khosla@stanford.edu, Mailing address: Department of Chemistry, Stanford University, Stanford, CA 94305-5080, Phone: 650-723-6538.
[§]Present address: Joule Unlimited, Inc., Cambridge, MA 02142

The benzoisochromanequinone (BIQ) antibiotic frenolicin B, produced by the actinomycete *Streptomyces roseofulvus*, has been extensively investigated as an anticoccidial agent owing to its potent activity against *Eimeria tenella* [6–9]. Nonetheless, low fermentation titers [10] and challenging synthetic procedures [11,12] appear to have limited further development of this promising anti-infective lead substance. We sought to address both of these problems by reconstructing a biosynthetic pathway to frenolicin B in the heterologous host *Streptomyces coelicolor* CH999, from which the entire actinorhodin biosynthetic gene cluster has been deleted [13].

Materials and Methods

General

S. coelicolor CH999/pBOOST* [14], which lacks the complete actinorhodin (*act*) gene cluster, was used as the host for production of polyketides. The plasmid pBOOST* has been shown to cointegrate with vectors containing the SCP2* origin of replication, thereby resulting higher copy numbers and correspondingly improved antibiotic titers[14]. The transformation of shuttle vectors bearing BIQ pathway genes into *S. coelicolor* CH999/pBOOST* were performed following standard proceedure[15]. Deuterated solvents for NMR experiments were purchased from Cambridge Isotope Laboratories, Inc. (Andover, MA) and all other solvents were purchased from Fisher Scientific (Pittsburgh, PA) at the highest available grade. ^{1}H and ^{13}C NMR spectra of purified polyketide products were recorded on Varian Inova 500 or 600 MHz instrument in CD$_3$OD or DMSO-d_6. The ^{1}H NMR spectra were referenced to the solvent peak at 3.31 ppm for CD$_3$OD or 2.50 ppm for DMSO-d_6. The ^{13}C NMR spectra were referenced to solvent at 49.0 ppm for CD$_3$OD or 39.52 for DMSO-d_6. Single-bond ^{1}H -^{13}C, multiple-bond ^{1}H - ^{1}H and ^{1}H -^{13}C connectivity was determined by HSQC, COSY and HMBC respectively on Varian Inova-600 NMR instrument. Mass spectra were obtained by electrospray ionization (ESI) at the Vincent Coates Foundation Mass Spectrometry Laboratory at Stanford University.

Construction of Shuttle Vectors

All cloning steps were performed in either *E. coli* XL1-Blue (Stratagene, La Jolla, CA), or *E. coli* DH5α (MCLab, South San Francisco, CA). Plasmids used for cloning included pUC18 (New England Biolabs, Ipswich, MA) and pET28b (Novagen, now EMD Bioscience, Madison, WI). Expression vectors were constructed using standard molecular biology techniques. See the supporting information for a detailed description of the primers and construction.

Production, Isolation, and Characterization of Polyketide Products

Each transformed strain was grown on R5 agar plates containing 50 mg/l thiostrepton and 100 mg/l of apramycin at 30°C for 7 days [15], after which metabolites were extracted with either 100% EtOAc or EtOAc/MeOH/Acetic Acid (89:10:1). This crude material was purified by a variety of methods including preparative HPLC and NaHCO$_3$ extraction. Structural determination was performed using a variety of 2D heteronuclear NMR experiments and LC/MS. See the SI for full details.

Toxoplasma gondii Growth Inhibition

Tachyzoites of *T. gondii* strain RH *hxgprt* YFP [16] were harvested from human foreskin fibroblast (HFF) monolayers grown in 25 cm^2 T-flasks. These parasites were then inoculated into a 96-well culture plate containing a confluent layer of HFF cells with ~8×10^3 tachyzoites/0.32 cm^2 well). Parasites were pre-incubated with HFF cells for 6h at 37 °C, 5% CO_2. After pre-incubation, the media was exchanged for fresh DMEM complete ((Dulbecco's modified eagle medium) supplemented with 1% PS (penicillin-streptomycin) and 10 % fetal bovine serum) containing a given concentration of antiparasitic agent. Cultures were then incubated for 72 hours at 37 °C, in 5% CO_2. Parasite growth inhibition was monitored in a SpectraMax Gemini EM fluorescent plate reader (Sunnyvale, CA) at 510 nm excitation and 540 nm emission. ED_{50}s were determined using GraphPad Prism (La Jolla, CA).

Cytotoxicity Assay

HFF cell cytotoxicity was determined using a MTS (3-(4,5-dimethylthiazol-2-yl)-5-(3-carboxylmethoxyphenyl)-2H-tetrazolium) assay (CellTiter 96 Aqueous One Solution Assay; Promega). HFF cells (2×10^3 cells/well) were grown in a 96 well plate until confluence (~48 hours) in phenol red free DMEM complete at 37 °C, 5% CO_2. Varying concentrations of antiparasitic agent were then added to each well and incubated for 48 hours at which point the medium was replaced with 100ul phenol red free DMEM and 20 ul MTS. After an additional 1.5 hrs of incubation at 37 °C, and the absorbance at 490nm was calculated and the ED_{50} was determined using GraphPad Prism (La Jolla, CA).

Results and Discussion

Determining the Tailoring Enzymes Necessary for BIQ Core Formation

Before embarking on the reconstruction of the frenolicin pathway, we first attempted to complete the biosynthesis of the simplest BIQ, deoxykalafungin **2a** (Scheme 1)[17], which does not require an initiation module and is an intermediate in the actinorhodin (**4**) pathway [18]. Previous studies have shown that introduction of the plasmid pRM5 (which encodes *act* KS/CLF, ACP, C-9 KR, ARO, and CYC genes; for details, see Scheme 1) into CH999 leads to the production of 3,8-dihydroxy-1-methylanthraquinone-2-carboxylic acid (DMAC) (**6a**) and aloesaponarin II (**7a**), as summarized in Table 1 [13,14]. The next step in BIQ production is stereoselective reduction of the C-3 ketone into an alcohol capable of cyclizing the third ring of the scaffold (Scheme 1 in red). To accomplish this, we cloned the C-3 ketoreductase gene, encoded by *act*VI-ORF1, onto pRM5, yielding the plasmid pJF6 (Table 1). As predicted, *S. coelicolor* CH999/pJF6/pBOOST* yielded **5a** after cyclization and loss of water (Figure S16) [5,19].

The next step in the pathway is enoyl reduction of **5a** followed by oxygenation. Mutants of the actinorhodin producing strain *S. coelicolor* A3(2), in which the enoyl reductase gene *act*VI-ORF2 has been inactivated, produce no actinorhodin, and mutants of the secondary enoyl reductase gene *act*VI-ORF4 produce only 18% of the actinorhodin of the native strain [20]. We therefore constructed two derivatives of pJF6, pCR66 and pCR67, harboring *act*VI-ORF2 and *act*VI-ORF2/*act*VI-ORF4, respectively (Table 1). The product profiles of

S. coelicolor harboring either plasmid was identical, and included **2a** as the next isolable intermediate (Figure S16). This finding has two interesting implications for BIQ biosynthesis. First, overexpression of *act*VI-ORF2 in a pRM5 derived vector obviates the need for a supplementary enoyl reductase in a heterologous system. Second, and more interestingly, the inferred product of the enoyl reductase reaction (Scheme 1 bottom left) was not observed, nor was there a large buildup of **5a**. It therefore appears that, although the *act* gene cluster harbors dedicated oxygenase genes [21,22], the *S. coelicolor* genome either has a non-specific oxygenase capable of catalyzing the same reaction, or that quinone formation proceeds spontaneously in air.

Production of Frenolicin B

Having identified the genes required to produce **2a** in *S. coelicolor* CH999/pBOOST*, we turned our attention to frenolicin B and analogs thereof. Whereas the minimal PKS responsible for frenolicin production has been previously defined [23], the initiation module and downstream tailoring enzymes have not yet been characterized. Intriguingly, homologs of the *act*VI-ORF1 and *act*VI-ORF2 genes are not known to exist in the frenolicin (*frn*) gene cluster [24]. In fact, constructs harboring all putative biosynthetic genes from the identified *frn* gene cluster failed to produce frenolicin or any related BIQ antibiotic (data not shown). In the face of insufficient genetic data, we hypothesized that the tailoring enzymes identified in production of **2a** could be functionally repurposed for the biosynthesis of longer chain analogs. To accommodate the longer alkyl priming chain, we replaced the octaketide *act* KS-CLF genes with the mixed octaketide/nonaketide *frn* KS-CLF genes, and also included the genes thought to encode the initiation module of the *frn* PKS.

The *frn* gene cluster harbors homologs of the genes encoding the well-characterized initiation module of the R1128 cluster [25]. Specifically, *frn*I is a homolog of *zhu*H, *frn*K is a homolog of *zhu*C, and *frn*J is a homolog of *zhu*N. These genes encode a homodimeric KS responsible for chain initiation, an acyl-ACP thioesterase (AATE), and a dedicated ACP for the initiation module, respectively. Co-expression of these three *frn* genes with the genes encoding the *frn* KS-CLF, the *frn*N ACP the *act* C-9 KR, the *act* ARO and the *act* CYC, as well as the *act*VI-ORF1 and *act*VI-ORF2 genes (pJF35; Table 1) yielded a mixture of butyryl-primed nonaketide derivatives that arise from off-path cyclization reactions (Figure S17). In addition, very small quantities of **2b** were also observed. Aside from **6b** the two other major shunt products were propyl analogs of the previously identified compounds dehydromutactin, and SEK34 [26–28]. They form either due to the inability of the *act* ARO to aromatize the first ring or the inability of the *act* CYC to form the second 6-membered ring (Scheme 1). Notwithstanding the relative abundance of these shunt products, the ability of *act*VI-ORF1 and *act*VI-ORF2 to replace the unidentified components of the frenolicin pathway underscores the potential for rational design of a biosynthetic scheme using a diverse PKS toolbox in the face of incomplete genetic information.

Analogs of Frenolicin B

With a route in hand to the bioactive natural product frenolicin B, we turned our attention to the rational design of biosynthetic analogs. Earlier work with *Eimeria tenella* had shown that extension of the C-15 methyl substituent of **1a** to a propyl substituent (**1b**) led to

improved antiparasitic activity.[6] We therefore reasoned that analogs **1c** and **1d** could be useful to investigate the steric effect of the C-15 substituent on biological activity. Because chemical synthesis of such analogs is not straightforward, we replaced the genes encoding the *frn* initiation module and ACP with homologs from the R1128 cluster, which incorporates bulkier primer units into the polyketide backbone [29]. At the same time, to compensate for the anticipated increase in overall chain length of the polyketide skeleton, we also replaced the *frn* KS-CLF genes with homologs from the decaketide tetracenomycin (*tcm*) PKS [30]. In combination with the *act* KR, *act* ARO, and *act* CYC, this hybrid bimodular PKS gene cluster yielded a mixture of compounds including **6c**, **6d**, **7c** and **7d** (pYT127; Table 1 and Figure S18) [23].

Further inclusion of the *act*VI-ORF1 and *act*VI-ORF2 genes yielded *S. coelicolor* CH999/ pJF9, which produced a spectrum of products including the desired **2c** and **2d** (Table 1 and Figure S18). Although this strain produced a wide range of uncharacterized polyketide products, the ratio of the desired products **2c** and **2d** to the shunt products **6c** and **6d** was considerably higher in this recombinant strain than in *S. coelicolor* CH999/pJF35/ pBOOST*. The lack of large quantities of butyl- and isopropyl-primed analogs of **8** and **9** indicate that *act* ARO and CYC interface with the *tcm* min PKS better than with the *frn* PKS. In addition, this suggests that substrate incompatibility arising from increased alkyl priming unit length is unlikely to be the cause of the large amounts of **8** and **9** observed in *S. coelicolor* CH999/pJF35/pBOOST*. These rationally designed analogs highlight the versatility of our approach to polyketide construction, and enabled evaluation of their antiparasitic activities.

Biological Evaluation against *Toxoplasma gondii*

Previous studies with *E. tenella* showed that the lactone forms of the BIQs **1a** and **1b** were more potent than the free acid forms (**2a** and **2b**) [6]. We therefore converted our isolated analogs **2a-d** into their corresponding lactones **1a-d** by previously reported methods [31]. The structures of the novel compounds **1c** and **1d** were confirmed by NMR and mass spectrometric analysis (Tables S3, S5 and S6). The compounds were assayed against *Toxoplasma gondii*, the causative agent of toxoplasmosis, along with the known antiparasitic agent pyrimethamine as a reference.[32] A slight modification of a previously reported yellow fluorescence protein reporter assay was used for this purpose [16] (Figures S1 and S2). As summarized in Table 2, within the C_1-C_4 range, the alkyl substituent has little effect on antiparasitic activity against *T. gondii*, but the longer branched substituent leads to a notable decrease in activity. Thus, the benefit of the longer substituent against *E. tenella* does not hold in our assays, and could be due to improved pharmacokinetics or differential species specificity. To assess their relative tolerability by mammalian cells, we also measured the cytotoxicity of **1a-d** against HFF-1 cells using a MTS-based assay (Figure S3). The therapeutic indices of **1a-d**, reported in Table 2, appear to be comparable.

Conclusion

In summary, notwithstanding incomplete genetic data for the natural product biosynthetic pathway, we have successfully engineered a chimeric, heterologous system for the

production of frenolicin B. Furthermore, we have exploited this heterologous system to produce novel frenolicin analogs that are difficult to access by alternative methods. Our results showcase the utility of a modular approach to the creation of medicinally relevant polyketide products of type II PKSs. Last but not least, we have shown that the new compounds have antiparasitic activity against *T. gondii in* vitro. Further modification of the biosynthetic system presented here could yield additional improvements in BIQ productivity as well as additional analogs of frenolicin B.

Supplementary Material

Refer to Web version on PubMed Central for supplementary material.

Acknowledgements

References

1. Khosla, C.; Ridley, CP. Encyclopedia of Microbiology. San Diego, CA: Academic Press; 2009. p. 472-481.

2. O'Hagan, D. The Polyketide Metabolites. Chichester, UK: Ellis Horwood; 1991.

3. Das A, Khosla C. Biosynthesis of aromatic polyketides in bacteria. Acc. Chem. Res. 2009; 42:631–639. [PubMed: 19292437]

4. Hertweck C. The biosynthetic logic of polyketide diversity. Angew. Chem., Int. Ed. 2009; 48:4688–4716.

5. Hopwood D, Taguchi T, Ebizuka Y, Ichinose K. A new mode of stereochemical control revealed by analysis of the biosynthesis of dihydrogranaticin in Streptomyces violaceoruber Tu 22. J. Am. Chem. Soc. 2001; 123:11376–11380. [PubMed: 11707113]

6. Omura S, Tsuzuki K, Iwai Y. Anticoccidal activity of frenolicin B and its derivatives. J. Antibiot. 1985; 38:1447–1448. [PubMed: 4066499]

7. Armer RE, et al. Anticoccidial activity of novel semi-synthetic analogues of deoxyfrenolicin and Frenolicin B (Part I). Heterocycl. Commun. 1998; 4:309–315.

8. Armer RE, et al. Anticoccidial activity of novel semi-synthetic analogues of deoxyfrenolicin and Frenolicin B (Part II). Heterocycl. Commun. 1998; 4:345–350.

9. Armer RE, et al. Carbocyclic frenolicin analogues: novel anticoccidial agents. Bioorg. Med. Chem. Lett. 1998; 8:139–142. [PubMed: 9871641]

10. Omura, S.; Iwai, Y.; Awaya, J.; Oiwa, R. Compound, frenolicin B which is useful as an antibiotic. US Patent. #4199514. 1980.

11. Masquelina T, Hengartnerb U, Streith J. Naphthopyranquinone antibiotics: novel enantioselective syntheses of frenolicin B and some of its stereoisomers. Helv. Chim. Acta. 1997; 80:43–58.

12. Brimble MA, Narin MR, Prabaharan H. Synthetic strategies towards pyranonaphthoquinone antibiotics. Tetrahedron. 2000; 56:1937–1992.

13. McDaniel R, Ebert-Khosla S, Hopwood D, Khosla C. Engineered biosynthesis of novel polyketides. Science. 1993; 262:1546–1550. [PubMed: 8248802]

14. Hu Z, Hopwood DA, Hutchinson CR. Enhanced heterologous polyketide production in Streptomyces by exploiting plasmid co-integration. J. Ind. Microbiol. Biotechnol. 2003; 30:516–522. [PubMed: 12827516]

15. Kieser, T.; Bibb, MJ.; Buttner, MJ.; Chater, KF.; Hopwood, DA. Practical Streptomyces Genetics. Norwich, UK: The John Innes Foundation; 2000. p. 472-481.

16. Gubbels MJ, Li C, Striepen B. High-throughput growth assay for Toxoplasma gondii using yellow fluorescent protein. Antimicrob. Agents Chemother. 2003; 47:309–316. [PubMed: 12499207]

17. Hoekesema H, Krueger WC, Kalifungin II. Chemical Transformations and the Absolute Configuration. J. Antibiot. 1976; 29:704–709. [PubMed: 956056]

18. Hopwood DA. Genetic contributions to understanding polyketide synthases. Chem. Rev. 1997; 97:2465–2497. [PubMed: 11851466]

19. Ichinose K, et al. Proof that the actVI genetic region of Streptomyces coelicolor A3(2) is involved in stereospecific pyran ring formation in the biosynthesis of actinorhodin. Bioorg. Med. Chem. Lett. 1999; 9:395–400. [PubMed: 10091691]

20. Taguchi T, et al. Chemical characterisation of disruptants of the Streptomyces coelicolor A3 (2) actVI genes involved in actinorhodin biosynthesis. J. Antibiot. 2000; 53:144. [PubMed: 10805574]

21. Okamoto S, Taguchi T, Ochi K, Ichinose K. Biosynthesis of actinorhodin and related antibiotics: discovery of alternative routes for quinone formation encoded in the act gene cluster. Chemistry & biology. 2009; 16:226–236. [PubMed: 19246012]

22. Kendrew SG, Hopwood DA, Marsh NG. Identification of a monooxygenase from Streptomyces coelicolor A3(2) involved in biosynthesis of actinorhodin: purification and characterization of the recombinant enzyme. J. Bacteriol. 1997; 179:4305–4310. [PubMed: 9209048]

23. Tang Y, Lee TS, Khosla C, Lee HY. Exploring the biosynthetic potential of bimodular aromatic polyketide synthases. Tetrahedron. 2004; 60:7659–7671.

24. Bibb MJ, Sherman DH, Omura S, Hopwood DA. Cloning, sequencing and deduced functions of a cluster of Streptomyces genes probably encoding biosynthesis of the polyketide antibiotic frenolicin. Gene. 1994; 142:31–39. [PubMed: 8181754]

25. Tang Y, Lee TS, Khosla C. Engineered biosynthesis of regioselectively modified aromatic polyketides using bimodular polyketide synthases. PLoS Biol. 2004; 2:227–238.

26. McDaniel R, Ebert-Khosla S, Hopwood DA, Khosla C. Engineered biosynthesis of novel polyketides: actVII and actIV genes encode aromatase and cyclase enzymes, respectively. J. Am. Chem. Soc. 1994; 116:10855–10859.

27. Zhang H, et al. Mutactin, a novel polyketide from Streptomyces coelicolor. Structure and biosynthetic relationship to actinorhodin. J. Org. Chem. 1990; 55:1682–1684.

28. Khosla C, et al. Genetic construction and functional analysis of hybrid polyketide synthases containing heterologous acyl carrier proteins. J. Bacteriol. 1993; 175:2197–2204. [PubMed: 8468280]

29. Marti T, Hu Z, Pohl NL, Shah aN, Khosla C. Cloning, nucleotide sequence, and heterologous expression of the biosynthetic gene cluster for R1128, a non-steroidal estrogen receptor antagonist. J. Biol. Chem. 2000; 275:33443–33448. [PubMed: 10931852]

30. Bibb MJ, Biró S, Motamedi H, Collins JF, Hutchinson CR. Analysis of the nucleotide sequence of the Streptomyces glaucescens tcmI genes provides key information about the enzymology of polyketide antibiotic biosynthesis. EMBO J. 1989; 8:2727–2736. [PubMed: 2684656]

31. Li T, Ellison RH. Stereoselective total synthesis of racemic kalafungin and nanaomycin A. J. Am. Chem. Soc. 1978; 78:6264–6265.

32. McCabe R, Oster S. Current recommendations and future prospects in the treatment of toxoplasmosis. Drugs. 1989; 38:973–987. [PubMed: 2693048]
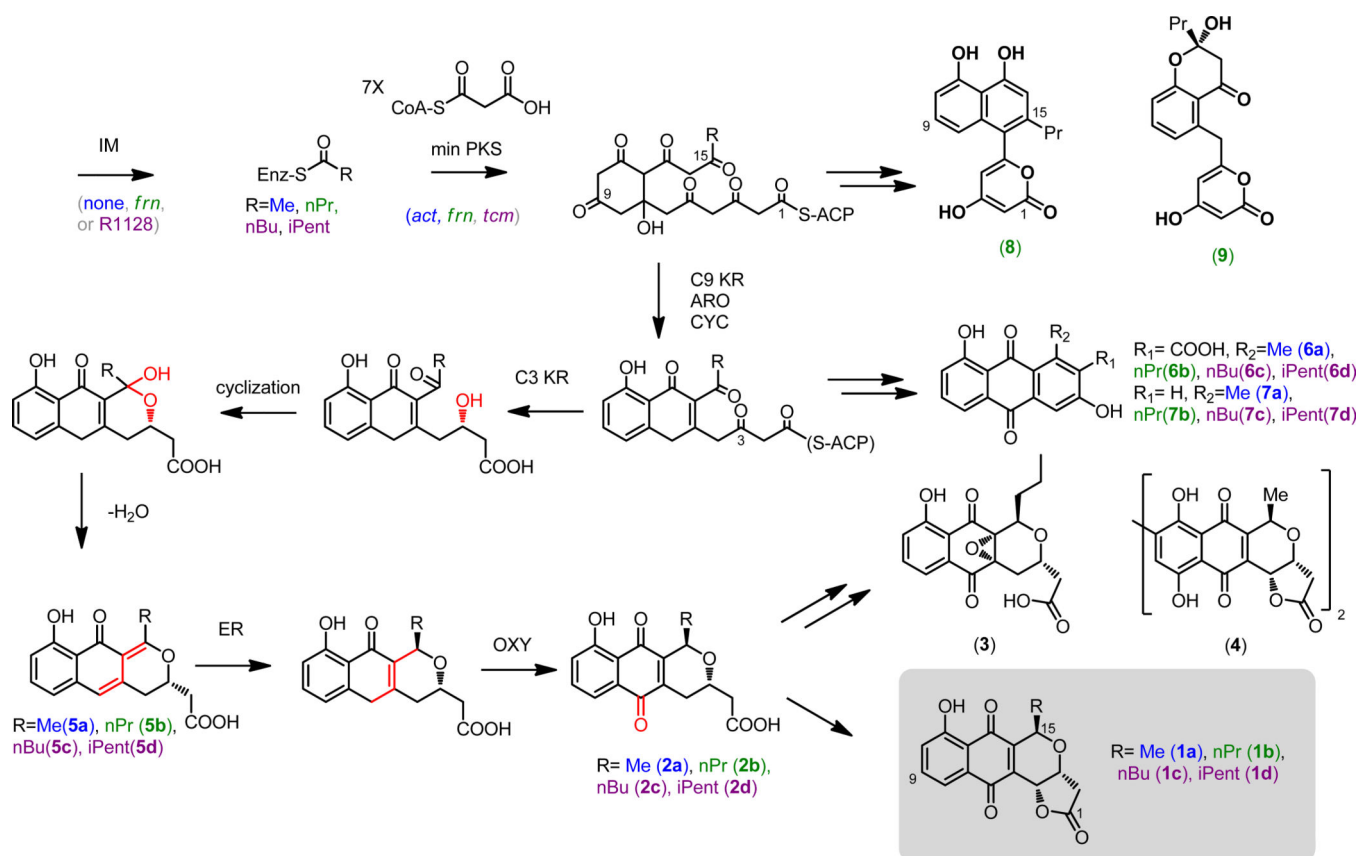
Scheme 1. A Biosynthetic Pathway to the Benzoisochromanequinones

The presumed biosynthetic route to **1a-d** is shown along with isolable intermediates and shunt products. Abbreviations: IM (initiation module = ketosynthase III, acyl carrier protein, acyl-ACP thioesterase); min PKS (minimal polyketide synthase = ketosynthase/chain length factor (KS/CLF), acyl carrier protein (ACP), malonyl-CoA:ACP transacylase (MAT)); C9 KR = C-9 ketoreductase encoded by *act*III; ARO = 1st ring aromatase encoded by *act*VII; CYC = 2nd ring cyclase encoded by *act*IV; C3 KR = C-3 ketoreductase encoded by *act*VI-ORF1; ER = enoyl reductase encoded by *act*VI-ORF2; OXY = oxygenase, encoded by an unidentified enzyme in the *S. coelicolor* genome. The natural product frenolicin A, (**3**) produced by *S. roseofulvus*, and the natural product actinorhodin, (**4**) produced by *S. coelicolor*, are also shown forming from their corresponding carboxylic acids, **2**. For details, see text.

Table 1

Plasmid Constructs and Resulting Polyketide Products

Plasmid[a]	KS-CLF	ACP	Initiation module	Other relevant PKS genes	Tailoring[c]	Polyketide Products[d]
pRM5[b]	*act*	*act*		*act* KR, *act* ARO, *act* CYC	*act*VB	**6a, 7a**
pJF6	*act*	*act*		*act* KR, *act* ARO, *act* CYC	*act*VI-ORF1, *act*VB	**5a, 6a, 7a**
pCR66	*act*	*act*		*act* KR, *act* ARO, *act* CYC	*act*VI-ORF1, *act*VI-ORF2, *act*VB	**2a, 5a, 6a, 7a**
pCR67	*act*	*act*		*act* KR, *act* ARO, *act* CYC	*act*VI-ORF1, *act*VI-ORF2, *act*VI-ORF4, *act*VB	**2a, 5a, 6a, 7a**
pJF35	*frn*	*frn*	*frn*	*act* KR, *act* ARO, *act* CYC	*act*VI-ORF1, *act*VI-ORF2, *act*VB	**2b, 6b, 8, 9**
pYT127[b]	*tcm*	R1128	R1128	*act* KR, *act* ARO, *act* CYC	*act*VB	**6c, 6d, 7c, 7d**
pJF7	*tcm*	R1128	R1128	*act* KR, *act* ARO, *act* CYC	*act*VI-ORF1, *act*VB	**5c, 5d 6c, 6d, 7c, 7d**
pJF9	*tcm*	R1128	R1128	*act* KR, *act* ARO, *act* CYC	*act*VI-ORF1, *act*VI-ORF2, *act*VB	**2c, 2d, 5c, 5d, 6c, 6d, 7c, 7d**

[a])Each pRM5 derived shuttle vector was introduced into *S. coelicolor* CH999/pBOOST* via transformation.

[b])Previously reported constructs (see text).

[c])Function of gene products: *act*VB flavin reductase; *act*VI-ORF1 C-3 ketoreductase; *act*VI-ORF2 enoyl reductase; *act*VI-ORF2 secondary enoyl reductase.

[d])See SI for compound characterization.

Table 2

Bioactivity of compounds 1a–d and pyrimethamine

Each compound was tested at least in triplicate. The therapeutic index is calculated by dividing the cytotoxic ED_{50} by the EC_{50} against *T. gondii*. See Figures S1 and S2 for growth inhibition curves.

Compound	T. gondii ED_{50} (nM)	HFF1 cytotoxicity ED_{50} (nM)	Therapeutic Index
1a	230 ± 15	5700 ± 800	25
1b	260 ± 15	2400 ± 300	9
1c	420 ± 30	-	-
1d	1200 ± 60	8000 ± 2000	7
Pyrimethamine	820 ± 60	>50000	>60